

Ensemble Enhanced Residual Network based Non-Contact Blood Pressure Estimation using CW Radar

Vuong Tri Tiep¹, Hoang Thi Yen^{1*}, Van-Phuc Hoang¹, Nguyen Huu Son², Chu Anh My¹, Guanghao Sun²

¹Le Quy Don Technical University, Hanoi, Vietnam

²The University of Electro-Communications, Tokyo, Japan

*Corresponding author: Hoang Thi Yen (Email: yenht@lqdtu.edu.vn)

Abstract—Continuous and unobtrusive blood pressure (BP) monitoring is essential for early detection and management of cardiovascular disorders. However, traditional solutions still rely on contact-based sensors or intermittent cuff measurements. This study proposes a deep learning framework for estimating systolic blood pressure (SBP) and diastolic blood pressure (DBP) using non-contact continuous-wave radar signals recorded under resting conditions. The method integrates a rigorous preprocessing pipeline, including artifact removal, phase reconstruction, feature normalization, and physiologically informed window extraction, with a data augmentation strategy designed to increase robustness against variability in radar micro-motion signals. Proposed one-dimensional Ensemble Enhanced Residual Network (EnE-ResNet) is developed to jointly regress SBP and DBP from four radar-derived feature channels (I, Q, phase, and magnitude). Evaluation on a publicly available resting-state radar dataset of 30 individuals demonstrates that the proposed approach achieves accurate BP estimation, with SBP and DBP mean absolute errors of 5.28 mmHg and 4.52 mmHg, respectively, and strong correlations with reference measurements. These findings highlight the potential of integrating radar sensing with deep learning to enable unobtrusive BP monitoring in future Internet of Medical Things (IoMT) applications.

Index Terms—Continuous-wave radar; blood pressure estimation; non-contact sensing; deep learning; EnE-ResNet.

I. INTRODUCTION

Continuous and cuff-less blood pressure (BP) monitoring has become increasingly important in modern healthcare, especially within the emerging Internet of Medical Things (IoMT) ecosystem. Conventional cuff blood pressure monitors, although clinically standardized, are discontinuously measuring, and incapable of capturing cardiovascular dynamics rapidly [1]. These limitations motivate research for non-contact, continuous BP estimation that are both unobtrusive and scalable. Microwave Doppler radar has recently gained significant attention as a promising modality due to its ability to acquire subtle chest-wall displacement, cardiac vibrations, and blood-flow-related micro-motions. Radar-based physiological sensing has demonstrated effectiveness in heart rate, respiration rate, and heart rate variability estimation [2-3]. Several studies have explored the feasibility of inferring BP from radar; however, existing approaches commonly rely on simplified preprocessing, handcrafted features, or direct mapping techniques that are vulnerable to phase noise, motion

artifacts, and inter-subject variability. Moreover, the complex and nonlinear relationship between radar I/Q dynamics and arterial pressure waveforms requires deep feature extraction mechanisms beyond the capacity of shallow models.

In recent years, deep learning techniques have been increasingly and effectively applied to cuffless blood pressure estimation, demonstrating superior capability in learning complex and nonlinear physiological relationships [4-6]. Accordingly, study [7] proposed the Temporal–Spatial Feature Fusion Network (TSFN) framework for radar signal, which integrates complementary neural components to enhance estimation accuracy. However, achieving clinical accuracy for radar-based blood pressure estimation remains a challenging research problem. Major difficulties arise from turbulence, multipath interference, environmental variability, and inherent inter-individual differences in vascular characteristics [7]. Related works have attempted to address these issues using advanced filtering, signal decomposition, or domain-specific transformation, but robust end-to-end BP estimation from short radar windows remains a challenging problem. Study [8] estimated blood pressure waveforms by proposed the MultiResLinkNet model, however, this study focused only on waveform estimation, and the authors concluded that subsequent research should incorporate a separate pathway within the framework to approximate BP amplitudes, including SBP and DBP. Additionally, data augmentation and ensemble learning, though effective in other biomedical tasks, have been underexplored in the context of radar-derived BP estimation.

To overcome these limitations, we propose a comprehensive deep learning framework that integrates robust preprocessing, feature engineering, and enhanced model design for accurate SBP and DBP estimation from contactless radar signals. The method begins with a strict cleaning pipeline, including consistency alignment of I/Q channels, removal of non-finite values, Savitzky–Golay filtering, phase reconstruction, magnitude derivation, and unified Z-score normalization. A sliding-window segmentation strategy is applied to extract physiologically valid radar segments, from which SBP and DBP are derived via waveform. To address data limitation and improve model generalization, we incorporate a multi-step data augmentation combining Gaussian noise injecting, time

shifting, and amplitude scaling. At the core of the proposed system is an improved ResNet architecture with bottleneck residual blocks, projection shortcuts, and dropout-enhanced fully connected layers designed for joint SBP-DBP regression. Furthermore, an ensemble learning strategy trains multiple independently shuffled models and aggregates their predictions, thereby mitigating overfitting and enhancing robustness. Through evaluation, the proposed radar-based BP estimation framework achieves low Mean Absolute Error (MAE), Root Mean Square Error (RMSE), and high correlation for both SBP and DBP, meeting key performance criteria of the British Hypertension Society (BHS) standard. These findings demonstrate that the combination of advanced preprocessing, augmentation, and proposed ensemble-enhanced ResNet (EnE-ResNet) architecture can significantly improve the reliability of radar-based BP estimation. The proposed approach contributes to the growing body of research supporting non-contact, continuous cardiovascular monitoring and highlights radar sensing as a viable modality for future IoMT-driven clinical applications.

The remainder of this paper is structured as follows. Section II provides details of proposed method of EnE-ResNet for BP estimation. Section III presents the publicly available datasets and benchmarking metrics used for model evaluation. Section IV shows the results of proposed method and section V discusses and concludes the research of radar-based BP monitoring in healthcare and IoMT system.

II. PROPOSED METHOD

The radar system employs a multiplier to mix the oscillator signal with the reflected, after which a low-pass filter (LPF) suppresses the high-frequency components, producing the I and Q channel signals as expressed in equations (1) and (2).

$$B_I(t) = A_r \cdot \cos \left(\frac{4\pi s(t)}{\lambda} - \frac{4\pi d_0}{\lambda} + \theta \right) \quad (1)$$

$$B_Q(t) = A_r \cdot \sin \left(\frac{4\pi s(t)}{\lambda} - \frac{4\pi d_0}{\lambda} + \theta \right) \quad (2)$$

where d_0 denotes the distance at time reference t_0 ; $s(t)$ is the body wall movement; $\theta = (-4\pi v t_0 / \lambda)$ and λ is the wavelength of the radar's transmitted signal.

The proposed method aims to estimate systolic and diastolic blood pressure (SBP and DBP) directly from short sequences of radar I/Q signals through a unified pipeline that integrates signal preprocessing, window segmentation, data augmentation, and a deep residual learning framework enhanced by ensemble prediction. The diagram of proposed method is shown in Figure 1.

Raw radar recordings are first subjected to a preprocessing procedure to ensure signal consistency and robustness. The in-phase (I), quadrature (Q), and blood pressure (BP) signals are aligned to a common length, and all non-finite samples are removed. When BP values are missing, interpolation is applied to restore continuity in the signal. To attenuate high-frequency noise while preserving morphological characteristics, I and

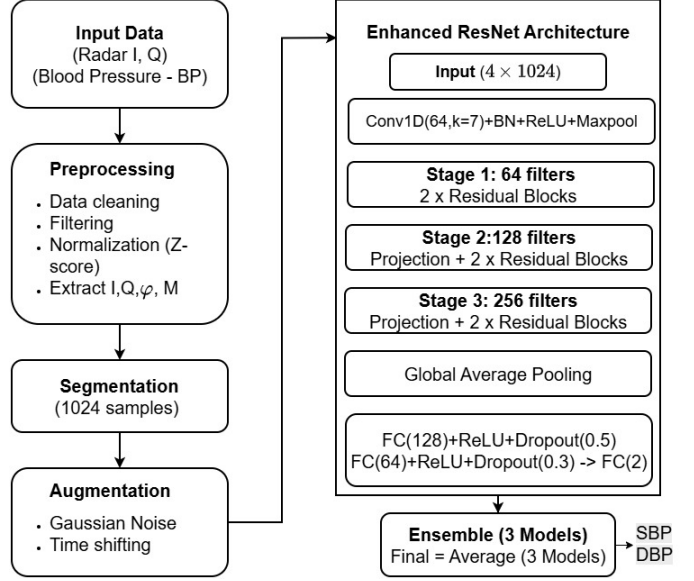


Fig. 1. Proposed EnE-ResNet based method for SBP and DBP estimation

Q signals are denoised using a Savitzky–Golay filter. Each channel is subsequently normalized using Z-score standardization to reduce inter-subject variability and stabilize model training. From the cleaned I and Q components, two additional features are derived, the instantaneous phase is computed as the arctangent of Q over I, and the signal magnitude is obtained from the Euclidean norm of the I/Q pair, as equations (3) and (4). These four complementary features capture both geometric and dynamic properties of the radar signal and constitute the multi-channel input to the neural network.

$$\varphi = \text{atan2}(Q\text{norm}, I\text{norm}) \quad (3)$$

$$M = \sqrt{(I\text{norm} + Q\text{norm})} \quad (4)$$

where $I\text{norm}$ is the normalized in-phase component, $Q\text{norm}$ denotes normalized quadrature component.

The continuous dataset is then transformed into supervised learning samples through a sliding-window segmentation strategy. Windows of 1024 samples are extracted, and each window is evaluated for physiological validity. The SBP and DBP labels are obtained by taking the maximum and minimum values of the BP waveform within each window, as shown in equations (5) and (6). Windows exhibiting unrealistically low BP variation or falling outside clinically acceptable ranges are discarded to prevent misleading training signals. This ensures that only high-quality, physiologically meaningful segments contribute to model development.

$$SBP_i = \max(ABP_i) \quad (5)$$

$$DBP_i = \min(ABP_i) \quad (6)$$

$$X_{augmented} = X_{original} + N(0, 0.02) \quad (7)$$

$$SBP_{final}(i) = (SBP_1(i) + SBP_2(i) + SBP_3(i)) / 3 \quad (8)$$

$$DBP_{final} = (DBP_1(i) + DBP_2(i) + DBP_3(i)) / 3 \quad (9)$$

To further improve model generalization in the presence of limited radar datasets, a multi-step data augmentation process is applied. For each window, three augmented versions are generated through random combinations of Gaussian noise injection, as equation (7), time shifting of 30 samples, and amplitude scaling by multiplying with a random coefficient in the range [0.95, 1.05]. This strategy expands the diversity of training examples and simulates realistic sources of variability. As a result, the augmented dataset better reflects the conditions encountered in real-world radar monitoring.

The core of the proposed framework is an one-dimensional enhanced Residual Network (ResNet) designed for joint regression of SBP and DBP, as shown in Figure 1. The network begins with a convolutional stem layer that extracts low-level temporal features. It then progresses through three residual stages with increasing filter sizes, each containing bottleneck-style residual blocks equipped with batch normalization, ReLU nonlinearities, and shortcut connections. Projections are introduced whenever the dimensionality changes, ensuring stable feature propagation across layers. After deep temporal representation learning, global average pooling aggregates the learned features, which are then processed through fully connected layers with dropout regularization to reduce overfitting. The output layer consists of $FC(2)$ for direct simultaneous prediction of SBP and DBP values, formulated as multi-target regression Output = [SBP, DBP] $\in \mathbb{R}^2$.

To enhance prediction stability and reduce model variance, an ensemble learning strategy is incorporated. Three independent networks with identical architectures are trained using differently shuffled training data. During inference, the outputs of all networks are averaged to produce the final BP estimates, as given in equations (8)-(9). By combining strong preprocessing, physiologically informed labeling, data augmentation, a deep residual architecture, and ensemble inference, the proposed method offers a robust and accurate solution for radar-based blood pressure estimation. The framework effectively captures subtle hemodynamic patterns encoded in radar signals while mitigating the inherent challenges associated with noise, inter-individual variability, and limited datasets.

III. DATA DESCRIPTION AND METRICS OF EVALUATION

A. DATA DESCRIPTION

The radar dataset employed in this study comprises raw CW radar recordings paired with reference arterial blood pressure waveforms, collected from 30 participants across five measurement conditions, with a total recording time of

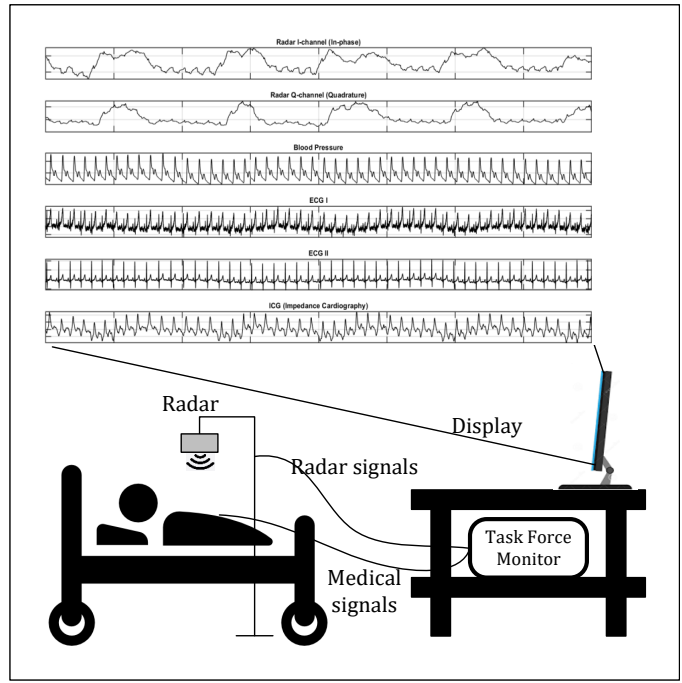


Fig. 2. Illustration of the data collection arrangement used in the dataset provided by Schellenberger et al. [9]

approximately 24 hours [9]. From this resource, only the resting condition was selected, as it offers stable physiological patterns suitable for training and validating a regression model without the confounding effects of strong hemodynamic perturbations. During the resting-condition measurements, each subject remained lied comfortably while a 24-GHz continuous-wave radar captured in-phase (I) and quadrature (Q) signals corresponding to subtle chest movements. These signals reflect subtle movements caused by cardiac activity and respiration. At the same time, a clinical-grade arterial pressure monitor captured continuous blood pressure waveforms, providing reliable reference values for systolic and diastolic pressure, as illustrated in Figure 2. Precise synchronization between the radar signal and the arterial blood pressure waveform ensures beat-to-beat correspondence, which helps train the data-driven model to learn the relationship between radar-based micro-motion features and underlying blood pressure dynamics.

B. METRICS OF EVALUATION

The performance of the proposed system was evaluated using four primary statistical metrics calculated separately for SBP and DBP. Mean Absolute Error (MAE) measures average prediction error magnitude in mmHg, as equation (10). RMSE is more sensitive to large errors due to its squared-error formulation. Pearson correlation coefficient R assesses linear relationship strength between predictions and ground truth, as given as equations (11) and (12). Standard deviation of error (STD) quantifies prediction consistency. Additionally, the British Hypertension Society (BHS) standard was applied, grading performance as A (excellent), B (good), C (acceptable), or D (inadequate) based on cumulative percentages of

predictions within ± 5 , ± 10 , and ± 15 mmHg thresholds. Grade A requires $\ge 60\%$, $\ge 85\%$, and $\ge 95\%$ within these thresholds respectively.

$$MAE = \frac{1}{N} \sum_{i=1}^N |BP_{pred}[i] - BP_{true}[i]| \quad (10)$$

$$RMSE = \sqrt{\frac{1}{N} \sum_{i=1}^N (BP_{pred}[i] - BP_{true}[i])^2} \quad (11)$$

where BP_{pred} is the estimated BP by proposed method on radar. BP_{true} is reference BP. N represents the number of test values.

$$R = \frac{\text{cov}(BP_{true}, BP_{pred})}{\sigma_{true} \cdot \sigma_{pred}} \quad (12)$$

where cov denotes covariance and σ represents standard deviation. R ranges from -1 to 1, with values closer to 1 showing stronger positive linear relationships.

$$Bias = \frac{1}{N} \sum_{i=1}^N (BP_{true}[i] - BP_{pred}[i]) \quad (13)$$

$$LoA = Bias \pm 1.96 \times SD_{diff} \quad (14)$$

Bland-Altman analysis was implemented to assess agreement, computing mean bias and limits of agreement (LoA), where narrow LoA indicates good consistency, as shown in (13) and (14). For the ensemble model, prediction confidence was quantified as the standard deviation across three models, with values lower than 3 mmHg indicating high reliability and bigger than 7 mmHg suggesting uncertain predictions requiring verification.

IV. RESULTS

The proposed framework was evaluated on the resting-state radar dataset after applying the complete preprocessing pipeline. An example of raw signal can be shown as Figure 3. A total of 3,809,734 valid samples were retained following data cleaning, from which 3,241 non-overlapping windows of 1,024 samples were extracted for model development (479

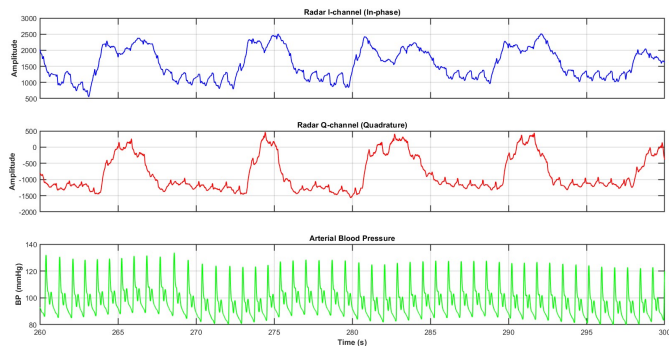


Fig. 3. Raw signal from radar and reference arterial blood pressure

windows were removed due to non-satisfactory physiological validity). After augmentation, the training corpus expanded to 3,564 sequences, which were subsequently divided into training ($n = 6,808$), validation ($n = 1,458$), and test ($n = 1,459$) sets. The blood pressure values associated with these sequences exhibited physiologically plausible distributions, with systolic blood pressure (SBP) averaging 132.9 ± 15.8 mmHg (range 97.2–158.3 mmHg) and diastolic blood pressure (DBP) averaging 88.4 ± 7.8 mmHg (range 70.1–101.6 mmHg).

The proposed EnE-ResNet model converged reliably during training, as reflected by steadily decreasing validation RMSE across epochs. When evaluated on the unseen test dataset, the ensemble demonstrated strong predictive performance for both SBP and DBP, as demonstrated in Figures 4 and 5. The scatter plots showed a strong correlation between the reference and predicted values, with $R = 0.94$ and $RMSE = 6.99$ mmHg for SBP, and $R = 0.87$ and $RMSE = 5.40$ mmHg for DBP, indicating that the model maintained high linearity and low error over the observed blood pressure range. The data points were concentrated near the ideal diagonal, reflecting the model's ability to track blood pressure variability quite accurately. The results of MAE are 5.28 mmHg and 4.52 mmHg for SBP and DBP, respectively.

Bland-Altman analysis further confirmed the reliability of the system as the SBP errors and DBP errors were mainly distributed within ± 1.96 SD of 11 mmHg and 8.8 mmHg respectively. Although the dispersion increased slightly at higher SBP and DBP levels, this trend was consistent with physiology and was common in non-invasive blood pressure estimation studies. The error distributions of both SBP and DBP were close to normal, with small mean errors (4.16 mmHg for SBP and 2.96 mmHg for DBP) and acceptable standard deviations, respectively. This indicates that the model performed stably, and maintained relatively consistent accuracy across the entire dataset.

Overall, the results indicate that the proposed model is capable of consistently and reliably estimating blood pressure under resting conditions, which meets the requirements for research on non-invasive blood pressure measurement using radar signals. Performance of proposed method in comparison with the BHS grading criteria, as shown in Table 1. For SBP, 56.6% of predictions fell within ± 5 mmHg of the reference, 85.4% within ± 10 mmHg, and 95.5% within ± 15 mmHg. The corresponding proportions for DBP were 56.7%, 96.6%, and 100.0%, respectively, indicating that DBP estimation meets Grade A requirements while SBP estimation approaches Grade B-A thresholds. Together, these results confirm that the proposed EnE-ResNet architecture, combined with carefully engineered preprocessing and augmentation strategies, enables accurate and reliable non-invasive blood pressure prediction from CW radar I/Q signals in resting conditions.

Our results demonstrate improved accuracy compared to previous studies in cuffless blood pressure estimation. The distributed errors achieved in our study (4.16 \pm 5.62 mmHg for SBP and 2.96 \pm 4.52 mmHg for DBP) show better performance than those reported in study [10] with 5.54 \pm 7.62 mmHg

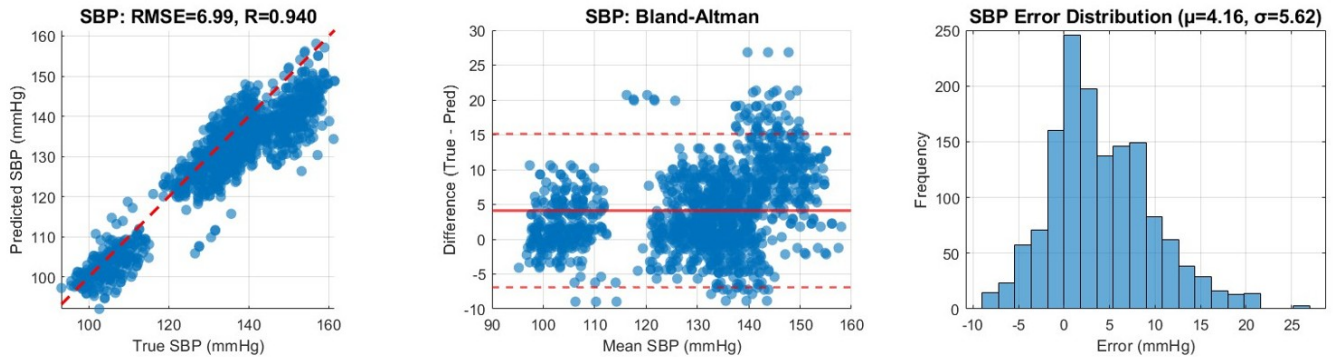


Fig. 4. Evaluation results for SBP estimation, including the correlation plot, Bland–Altman plot, and error distribution histogram

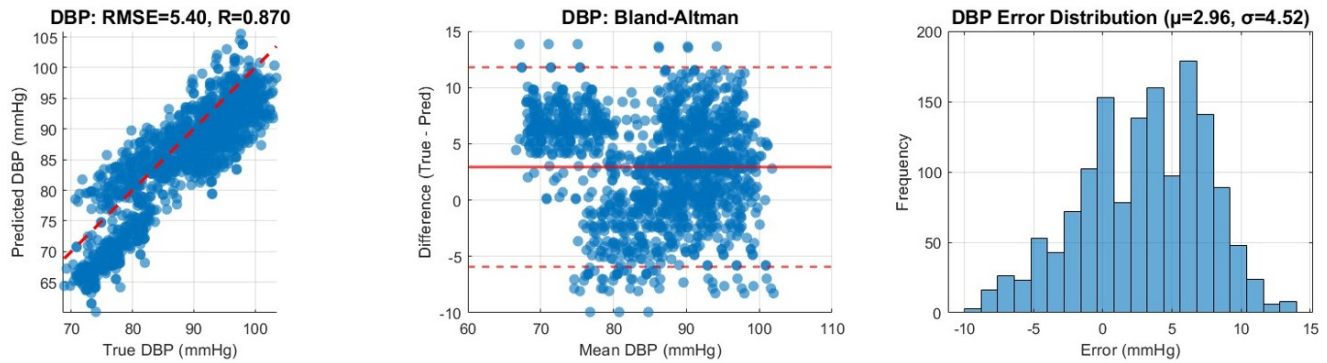


Fig. 5. Evaluation results for DBP estimation, including the correlation plot, Bland–Altman plot, and error distribution histogram

TABLE I
PERFORMANCE OF PROPOSED METHOD IN COMPARISON WITH THE BHS CRITERION

Method	Type	within ± 5 (mmHg)	within ± 10 (mmHg)	within ± 15 (mmHg)	
BHS	Grade A	60%	85%	95%	
	Grade B	50%	75%	90%	
	Grade C	40%	65%	85%	
Our results	SBP	56.6%	85.4%	95.5%	GradeA-B
	DBP	56.7%	96.6%	100%	GradeA

for SBP and 4.68 ± 6.16 mmHg for DBP. Additionally, our RMSE values of 6.99 mmHg for SBP and 5.40 mmHg for DBP indicate enhanced precision compared to study [11], which achieved an RMSE of 7.13 mmHg for continuous blood pressure amplitude estimation. Furthermore, the Pearson correlation coefficients obtained in our study ($R=0.94$ for SBP and $R=0.87$ for DBP) demonstrate stronger linear relationships between predictions and ground truth values than those reported in study [12] ($R=0.838$ for SBP and $R=0.797$ for DBP). These improvements suggest that our proposed EnE-ResNet based approach more reliable blood pressure estimation across both SBP and DBP measurements.

V. DISCUSSION

This study demonstrates that DBP estimation showed higher correlation and lower prediction error than SBP. This suggests that DBP is less sensitive to short-term mechanical disturbances and rapid cardiovascular changes, and therefore can be estimated more reliably from radar-based signals. The stable



Fig. 6. Hardware architecture integrating non-contact radar sensing and reference contact sensors for multimodal physiological data acquisition in our Laboratory

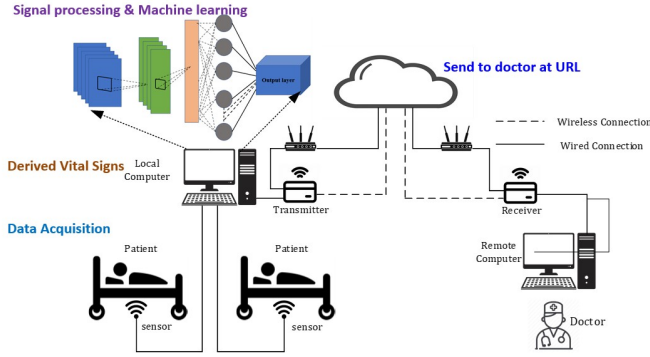


Fig. 7. Summary of our achieved system capabilities and future objectives, including real-time vital-sign monitoring and planned enhancements for blood pressure estimation

performance observed on the test sequences further highlights the effectiveness of the proposed preprocessing and data augmentation strategies. The removal of unstable signal segments, enforcement of physiological constraints, and expansion of the training distribution via noise injection and temporal shifting substantially enhanced model robustness. Moreover, the ensemble learning strategy helped reduce model variance and mitigate overfitting, which is particularly beneficial given the limited size of the available dataset.

Despite these promising outcomes, several limitations must be acknowledged. First, the study relied on resting-condition recordings, where subjects remained relatively motionless. While this choice ensured cleaner training data and reduced confounding variables, it does not fully reflect real-world circumstance in daily activities, where motion artifacts and changes in posture can significantly influence radar signatures. Second, the dataset originates from a controlled environment with a moderate number of participants; thus, the diversity of physiological patterns is limited. Broader population studies, including individuals with hypertension or cardiovascular abnormalities, would be necessary to evaluate clinical applicability. Additionally, radar signals are inherently sensitive to small positional changes and surrounding reflectors. Although data augmentation partially mitigates these effects, personalized calibration strategies may be required for deployment in uncontrolled environments.

VI. CONCLUSION

In conclusion, this work provides evidence that CW radar-based contactless blood pressure estimation is feasible and effective when combined with an appropriately structured deep learning framework. The proposed preprocessing pipeline, ensemble-based residual network architecture, and physiologically informed design collectively enable robust estimation of SBP and DBP under resting conditions, without direct skin contact.

Our future work will focus on developing a hardware system that integrates both a non-contact radar sensor and reference contact-based sensors to enable large-scale data acquisition

from healthy individuals and patients with cardiovascular conditions. Figure 6 illustrates the hardware prototype currently being refined by our research group, while Figure 7 summarizes the results achieved to date and the long-term objectives of the project. Notably, real-time measurement of non-contact vital signs, such as respiration rate, heart rate, and heart rate variability, has already demonstrated promising performance, and these results have been transmitted to clinicians through a real-time URL-based interface. The next phase of development will emphasize advancing vital sign estimation, particularly for blood pressure. Once the predictive models reach clinically acceptable accuracy, we will explore strategies to optimize the model structure to ensure efficient real-time deployment within IoMT applications.

ACKNOWLEDGMENT

This research is funded by Vietnam National Foundation for Science and Technology Development (NAFOSTED) under grant number 102.04-2025.36. We would like to thank NICT, Japan for supporting some research equipment and facilities under the ASEAN IVO project “Artificial Intelligence Powered Comprehensive Cyber-Security for Smart Healthcare Systems (AIPOSH)”.

CONFLICT OF INTEREST STATEMENT

The authors declare that they have no conflict of interest.

REFERENCES

- [1] Hu, Jiun-Ruey, et al. "Validating cuffless continuous blood pressure monitoring devices." *Cardiovascular digital health journal* 4.1 (2023): 9-20.
- [2] Iwata, Itsuki, et al. "Accurate Radar-Based Heartbeat Measurement Using Higher Harmonic Components." *IEEE Access* (2025).
- [3] Yen, Hoang Thi, et al. "Non-contact estimation of cardiac inter-beat interval and heart rate variability using time-frequency domain analysis for CW radar." *IEEE Journal of Electromagnetics, RF and Microwaves in Medicine and Biology* 7.4 (2023): 457-467.
- [4] Ibtehaz, Nabil, et al. "PPG2ABP: Translating photoplethysmogram (PPG) signals to arterial blood pressure (ABP) waveforms." *Bioengineering* 9.11 (2022): 692.
- [5] Harfiya, Latifa Nabila, Ching-Chun Chang, and Yung-Hui Li. "Continuous blood pressure estimation using exclusively photoplethysmography by LSTM-based signal-to-signal translation." *Sensors* 21.9 (2021): 2952.
- [6] Mahmud, Sakib, et al. "NABNet: a nested attention-guided BiConvLSTM network for a robust prediction of blood pressure components from reconstructed arterial blood pressure waveforms using PPG and ECG signals." *Biomedical Signal Processing and Control* 79 (2023): 104247
- [7] Wang, Pengfei, et al. "A Temporal-Spatial Feature Fusion Network for Accurate Non-Contact Blood Pressure Measurement via Radar." *IEEE Sensors Journal* (2025).
- [8] Chowdhury, Farhana Ahmed, et al. "Deep learning-based beat-to-beat arterial blood pressure estimation using distant radar signals." *Neural Computing and Applications* (2025): 1-26.
- [9] Schellenberger S, Shi K, Steigleider T, Malessa A, Michler F, Hameyer L, Neumann N, Lurz F, Weigel R, Ostgathe C, Koelpin A (2020) A dataset of clinically recorded radar vital signs with synchronised reference sensor signals. *Sci Data* 7:291.
- [10] Geng, Fanglin, et al. "Contactless and continuous blood pressure measurement according to caPTT obtained from millimeter wave radar." *Measurement* 218 (2023): 113151.
- [11] Ma, Ketao, Yiyuan Zhang, and Baohua Shan. "A Novel Contactless Approach to Continuous Blood Pressure Monitoring Using Complex CEEMDAN and Neural Networks." *IEEE Access* (2025).
- [12] Qiu, Ye, et al. "Non-contact blood pressure estimation from radar signals by a stacked deformable convolution network." *IEEE Journal of Biomedical and Health Informatics* 28.8 (2024): 4553-4564.